

Shapes of hydrophobic thick membranes

Trinh X. Hoang,^{1,2} Jayanth R. Banavar,¹ and Amos Maritan³

¹*Department of Physics, University of Maryland, College Park MD 20742, USA*

²*Institute of Physics, Vietnam Academy of Science and Technology, 10 Dao Tan, Hanoi 10000, Vietnam*

³*Dipartimento di Fisica ‘G. Galilei’, Università di Padova & CNISM, unità di Padova & INFN, sezione di Padova, Via Marzolo 8, 35131 Padova, Italy*

We introduce and study the behavior of a tethered membrane of *non-zero thickness* embedded in three dimensions subject to an effective self-attraction induced by hydrophobicity arising from the tendency to minimize the area exposed to a solvent. The phase behavior and the nature of the folded conformations are found to be quite distinct in the small and large solvent size regimes. We demonstrate spontaneous symmetry-breaking with the membrane folding along a preferential axis, when the solvent molecules are small compared to the membrane thickness. For large solvent molecule size, a local crinkling mechanism effectively shields the membrane from the solvent, even in relatively flat conformations. We discuss the binding/unbinding transition of a membrane to a wall that serves to shield the membrane from the solvent.

INTRODUCTION

The structure and dynamics of sheets or surfaces are important in diverse contexts in everyday life, in cell biology, in field theory and quantum gravity, and in condensed matter physics [1, 2]. Previous studies have concentrated on idealized surfaces - the thickness is neglected principally to facilitate an analytical approach (see the excellent work by David, Duplantier, Gutter and Wiese, reviewed in Ref.[3]) or partially captured by tethering together, in a two dimensional array, hard spheres, whose diameter equals the surface thickness. In the latter case, both the steric and interactions induced by the environment or solvent are modeled as standard two-body potentials which become singular (Dirac delta function) interactions in the continuum limit [4]. In this limit, self-interacting manifolds, in 1 dimension corresponding to a polymer chain and in 2 dimensions corresponding to a membrane, the subject of our study, cannot be correctly described by two body interactions [4]. The difficulty arises because a pair-wise interaction can only depend on the distance between the two parts of the manifold. One is unable to account for whether these two parts are near each other just because they lie on adjacent parts of the manifold or whether they are distant along the manifold and thence truly interacting. One could cure this problem by introducing some microscopic cut-off such that nearby parts of the manifold, at a distance smaller than this cut-off along the manifold, are defined to be non-interacting. This procedure is expected not to affect the long distance behavior but it affects many important intermediate scale effects of interest.

Extensive studies [5–7] have shown that there are vastly different behaviors between a conventional polymer modeled as a chain of non-overlapping spheres and a tube due distinct symmetries in the two cases. The latter can be imagined as a chain of coins whose symmetry is cylindrical. Self-avoidance of a flexible tube can be imposed by using a three-body potential [8]. A tube

subject to maximal compaction takes on the geometry of an optimal helix [5], whose local curvature is equal to the tube thickness. Strikingly, this geometry is adopted by α -helices in proteins. On the other hand, a fcc lattice is an optimal arrangement for a chain of spheres subject to compaction, provided the tether constraints do not conflict with this arrangement. Surprisingly, chains of overlapping spheres [9] behave in a manner akin to a tube. This is because the overlap between adjacent spheres along the chain result in a loss of spherical symmetry and endow an anisotropy to the chain much as a tube does [10].

The principal theme of this paper is to introduce a model of a thick hydrophobic membrane that encapsulates the correct symmetry associated with its intrinsic two dimensional nature. The implementation of the non-zero thickness of the membrane is carried out through a four-body potential [4]. Unlike the model of tethered spheres, the membrane thickness in our model provides a length scale that is independent of the discretization of the membrane surface, and thus is free of the singularity problem in the continuum limit. The interaction with the solvent molecules is captured through Hadwiger’s theorem [11] as explained in [12]: the effective self-interactions of the membrane, induced by a short-range solvent-membrane potential, can have only four distinct contributions. Two of these interactions are proportional to the integrals of the mean curvature and Gaussian curvature over the entire surface. The other two interactions pertain to an entropic contribution arising from the volume excluded to the solvent molecules [13] and an energy contribution measured by the area of the membrane that is exposed to the solvent molecules. The membrane thickness already takes into account the mean curvature effects because, at each position on the surface, the curvature radii have to be larger than the thickness itself. The integral of the Gaussian curvature is constant if the membrane topology is kept fixed. Furthermore, because the membranes we consider are open,

the volume excluded to the solvent molecules is partly taken into account by the buried area or equivalently by its complement, the exposed area. Thus our focus here is on understanding how the area of the membrane exposed to the solvent molecules influences the nature of the conformations of a hydrophobic membrane immersed in a solvent. We show that distinct behaviors are obtained for different ratios between the membrane thickness and the solvent molecule size, both in the absence and presence of an inert wall, which serves to shield one side of the membrane from the solvent. We find several familiar conformations that have not been observed in previous studies of conventional models.

MATHEMATICAL DESCRIPTION OF THICK MEMBRANE

The notion of thickness can be introduced for a continuum surface in 3-D. The position vector of a point on the surface is given by $\mathbf{r}(\vec{s})$, where $\vec{s} = (s^1, s^2) \in \mathcal{D}$ defines the local (curvilinear) coordinate frame on the surface. The two tangent vectors are

$$\partial_i \mathbf{r}(\vec{s}) \equiv \frac{\partial \mathbf{r}(\vec{s})}{\partial s^i}, \quad i = 1, 2. \quad (1)$$

The square of the distance between two neighboring positions on the surface, \vec{s} , $\vec{s} + d\vec{s}$ is given by

$$d\mathbf{r}^2 = g_{ij} ds^i ds^j, \quad (2)$$

where

$$g_{ij} \equiv \partial_i \mathbf{r}(\vec{s}) \cdot \partial_j \mathbf{r}(\vec{s}), \quad (3)$$

is the metric tensor. We will assume that the tangent vectors are linearly independent at all points on the surface which is equivalent to

$$\left(\partial_1 \mathbf{r}(\vec{s}) \times \partial_2 \mathbf{r}(\vec{s}) \right)^2 = \det(g_{ij}) \equiv g \neq 0. \quad (4)$$

The surface element at position \vec{s} is given by

$$d\mathcal{S}(\vec{s}) \equiv d^2s \sqrt{g(\vec{s})}. \quad (5)$$

We also assume that the local coordinate frame is chosen such that the normal to the surface

$$\hat{\mathbf{n}}(\vec{s}) = \frac{\partial_1 \mathbf{r}(\vec{s}) \times \partial_2 \mathbf{r}(\vec{s})}{|\partial_1 \mathbf{r}(\vec{s}) \times \partial_2 \mathbf{r}(\vec{s})|}, \quad (6)$$

is always on one side of the surface. If the thickness of the surface is 2Δ , then the radius of the sphere tangent at $\mathbf{r}(\vec{s})$ and going through another point $\mathbf{r}(\vec{t})$ on the surface (\vec{t} is a vector in the curvilinear coordinates),

$$\mathcal{R} = \frac{[\mathbf{r}(\vec{t}) - \mathbf{r}(\vec{s})]^2}{2\hat{\mathbf{n}}(\vec{s}) \cdot [\mathbf{r}(\vec{t}) - \mathbf{r}(\vec{s})]}, \quad (7)$$

cannot be smaller than Δ for all \vec{s} and \vec{t} (fig. 1).

For a triangulated surface with fixed connectivity corresponding to the middle surface of a membrane, assume that the vertices are denoted as $i, j, k \dots$ whose positions are given by $\mathbf{r}_i, \mathbf{r}_j, \mathbf{r}_k \dots$. A triangle of vertices i, j , and k is denoted by (ijk) . For each triangle (ijk) , we assign an orientation such that for the completely flat surface the normal vector

$$\hat{\mathbf{n}}_{ijk} = \frac{(\mathbf{r}_j - \mathbf{r}_i) \times (\mathbf{r}_k - \mathbf{r}_i)}{|(\mathbf{r}_j - \mathbf{r}_i) \times (\mathbf{r}_k - \mathbf{r}_i)|} \quad (8)$$

always points in the same, say up, direction. The thickness is defined in analogy with the continuum case. The radius of the sphere tangent to the triangle (ijk) at its center of mass $\mathbf{r}_{ijk} \equiv (\mathbf{r}_i + \mathbf{r}_j + \mathbf{r}_k)/3$ and going through the node \mathbf{r}_m ,

$$\mathcal{R}_{ijkm} = \frac{(\mathbf{r}_m - \mathbf{r}_{ijk})^2}{2|\hat{\mathbf{n}}_{ijk} \cdot (\mathbf{r}_m - \mathbf{r}_{ijk})|}, \quad (9)$$

is constrained to be greater than or equal to $\Delta \forall (ijk), m \neq i, j, k$.

EXPOSED AREA OF THICK MEMBRANE

Assume that the solvent molecule is a spherical paint brush of radius R (fig. 1). The exposed area of a membrane is defined as the membrane's surface area accessible by this spherical paint brush. Each membrane has two sides, + and -, defined by two triangulated surfaces, \mathcal{S}_+ and \mathcal{S}_- , at a distance Δ from the middle surface. We assign a normal to each node \mathbf{r}_i of the middle surface as the *average* normal of all the triangles sharing the i -th node:

$$\hat{\mathbf{n}}_i = \frac{\sum_{jk} \hat{\mathbf{n}}_{ijk}}{|\sum_{jk} \hat{\mathbf{n}}_{ijk}|}, \quad (10)$$

where the sum is over all oriented triangles sharing the i -th node. The number of such triangles is six in the bulk and less than six at the boundary. Each $\hat{\mathbf{n}}_i$, by definition, is oriented in the direction of \mathcal{S}_+ . Thus we define the nodes of the surfaces \mathcal{S}_\pm as

$$\mathbf{p}_i^\pm = \mathbf{r}_i \pm \Delta \hat{\mathbf{n}}_i. \quad (11)$$

To calculate the exposed area of the surfaces \mathcal{S}_\pm , one places a sphere of radius R tangentially to each triangle on the surfaces \mathcal{S}_\pm at its center of mass, and then to check whether the sphere overlaps with any of the other points on these two surfaces. If there is no overlap the triangle is said to be exposed to the solvent. The following quantity can be calculated for each triangle (ijk) in the \mathcal{S}_\pm surfaces:

$$B_{ijk}^\pm = \min_{m\lambda} |\mathbf{p}_{ijk}^\pm \pm R \hat{\mathbf{N}}_{ijk}^\pm - \mathbf{p}_m^\lambda|, \quad (12)$$

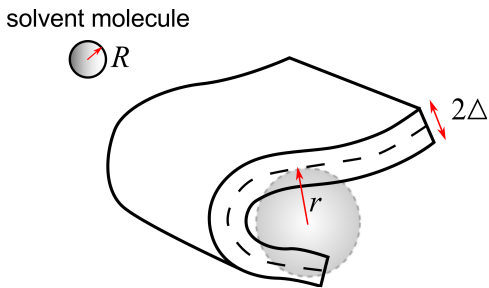


FIG. 1: Cartoon of a thick membrane and a solvent molecule. Each side of the membrane is at a distance Δ from the middle surface (dashed line). Self-avoidance requires that any sphere tangent to the middle surface at one point and passing through another point on this surface must have a radius $r \geq \Delta$. The solvent molecule is considered as a spherical paint brush of radius R . The membrane exposed surface area is defined as the area on both side of the membrane that is accessible to that spherical paint brush.

where \mathbf{p}_{ijk}^\pm and $\hat{\mathbf{N}}_{ijk}^\pm$ is the center of mass and the normal of that triangle, respectively, and λ can be + or -. The exposed areas in the surfaces \mathcal{S}_\pm are defined as

$$\Sigma_\pm = \frac{1}{2} \sum_{(ijk)} |(\mathbf{p}_j^\pm - \mathbf{p}_i^\pm) \times (\mathbf{p}_k^\pm - \mathbf{p}_j^\pm)| \Theta[R - B_{ijk}^\pm], \quad (13)$$

where $\Theta()$ is the step function, and the sum is taken over all triangles on a given surface.

MODEL OF THICK HYDROPHOBIC MEMBRANE

Following standard practice, here we model the thick membrane as a set of points forming a triangular lattice representing the membrane's middle surface. The links on the lattice are fixed and have lengths that are allowed to vary freely between $0.9l$ and $1.1l$, where l is the unit length. Self-avoidance is implemented through an effective four-body potential (Eq.(9)) to ensure the membrane thickness of 2Δ . Due to the effects of discretization, this procedure is accurate as long as $\Delta/l \geq 0.5$. Note that Δ provides a length scale that is independent of the discretization length l . The continuum limit can be approached by decreasing l while keeping Δ constant.

We consider a membrane that is hexagonal in shape when it is perfectly flat with the edge length of L . The solvent molecule is modeled as a spherical paint brush with radius R . The interaction between solvent molecules is not considered in our study and yields a higher order correction. For a hydrophobic solvent, there is a tendency to minimize the exposed area by appropriate folding of the membrane, which, at non-zero temperatures, is counteracted by an entropic contribution promoting relatively flat conformations. An effective self-attraction is

thus introduced through a potential energy:

$$E = (\varepsilon/l^2)(\Sigma^+ + \Sigma^-), \quad (14)$$

where ε provides an energy unit and Σ^\pm are the exposed areas of the + and - sides, respectively.

Monte Carlo simulations are carried out to study the behavior of the membrane at various temperatures. In a Monte Carlo move, one node in the triangulated lattice of the membrane's middle surface is selected and displaced in a random direction by a random displacement. The magnitude of the displacement is constrained to be less than 10% of the lattice constant l . The move is rejected immediately if (1) a new bond length on the lattice due the displacement is smaller than $0.9l$ or larger than $1.1l$, or (2) the membrane thickness constraint is violated. Otherwise, the move is accepted with probability $P = \min[1, \exp(-\Delta E/k_B T)]$, where T is temperature, and ΔE is a change in the effective energy. A parallel tempering scheme with 16 to 20 replicas is adopted to get efficient sampling of the conformational space.

LARGE VS. SMALL SOLVENT SIZE

Figs. 2 show typical conformations of a membrane in the large and small solvent size regimes. At high temperatures, the entropy dominates, there is no tendency for minimizing the area exposed to the solvent, and the conformations in both regimes are flat. On lowering the temperature, the membranes tend to become compact by minimizing their exposed area to the solvent but their behaviors are remarkably different for the two cases of small and large solvent molecule sizes. The correlations between the normal vectors of the membranes also show a major difference between the low temperature conformations in the large and small solvent regimes (Fig. 3).

When R is larger than Δ , the low temperature phase is crinkled and contains many different conformations. The crinkling is essentially a local deformation that does not violate the local bending constraint of a thick membrane yet excludes the large paint brush from accessing the surface. Locally, below the persistence length, the membrane is *essentially flat* yet crinkled. At the lowest temperature, the crinkled conformations are almost completely buried (Fig. 2a). We have verified that, for the same solvent-induced energy function, the impenetrable plaquette model [14], behaves similarly to the thick membrane in the large solvent molecule limit - i.e. the thickness is not relevant when the solvent molecules are large. Interestingly, for large solvent size, the local crinkling mechanism induces a stiffening of the membrane in the flat phase (Fig. 3).

When R is considerably smaller than Δ , the membrane exhibits a transition from the high temperature flat phase to the low temperature folded phase characterized

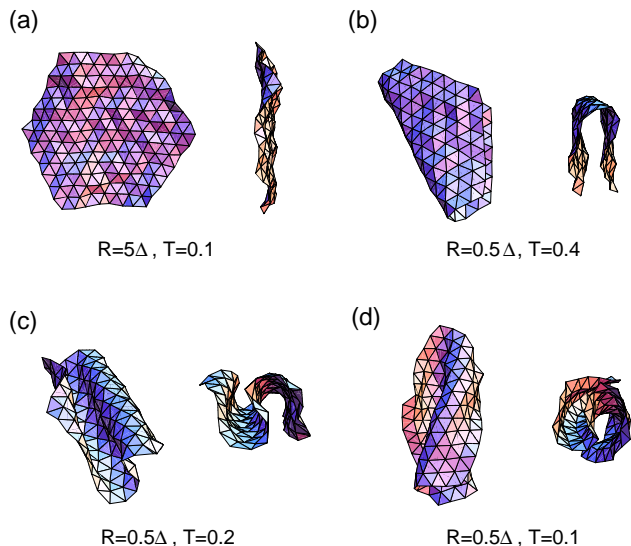


FIG. 2: Conformations of a hydrophobic membrane immersed in water. The membrane has an edge length of $L = 7l$ and the thickness $2\Delta = 1.6l$. (a) Two views of a conformation found at $T = 0.1\epsilon/k_B$ for a membrane when the solvent radius, $R = 5\Delta$, is large. The triangular lattice shown indicates the membrane's middle layer. The membrane is fully buried due to the local crinkling mechanism. Note the the membrane surface is rough but the overall shape is flat. (b–d) Three typical folded conformations at low temperatures for a membrane in the small solvent regime. The solvent radius is $R = \Delta/2$, and the temperatures are $T = 0.4\epsilon/k_B$ (b), $0.2\epsilon/k_B$ (c), and $0.1\epsilon/k_B$ (d) as indicated. The buried fractions are 0.31, 0.37 and 0.44 for the three cases (b, c, d), respectively. Note that folding occurs predominantly along one axis.

by a few different folded geometries (Fig. 2b,c,d). The membrane undergoes a spontaneous symmetry breaking within the plane of the membrane. The folding of the membrane occurs multiple times along a dominant folding axis.

RIBBONS IN 2-D

We have carried out also simulations of solvophobic ribbons in 2- D (Fig. 4). The ribbons have a thickness of 2Δ and the solvent molecule in this case is considered as circular disc of radius R . We consider a discretized ribbon axis described by a set of equally spaced points separated by $b = \Delta/2$. The self-avoidance constraint is imposed by requiring that none of the radii of the circles passing through each of the triplets of the points on the ribbon axis is smaller than Δ . All triplets of points are considered. Like for membranes, we found two regimes related to the solvent size. For $R > \Delta$, the ground state of the ribbon is a straight conformation with local crinkling (Fig. 4a). For $R \leq \Delta$, one finds folded conformations with some local crinkling on the outer perimeter (Fig. 4 b,c). The folded conformations of the ribbon

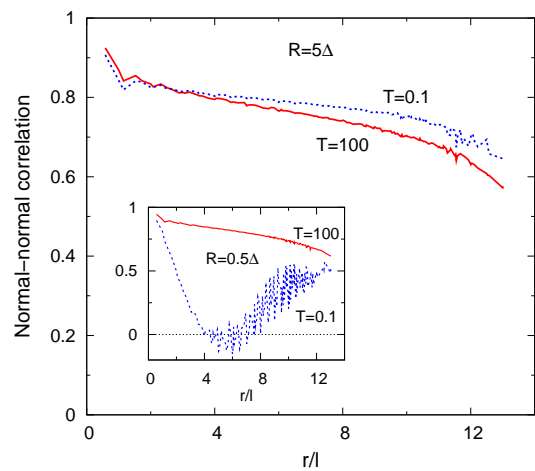


FIG. 3: Correlation between normal vectors. Dependence of the correlation between normal vectors, $\langle \mathbf{n}_x \mathbf{n}_{x+r} \rangle - \langle \mathbf{n}_x \rangle \langle \mathbf{n}_{x+r} \rangle$, on r , the distance between them, are shown for the large solvent ($R = 5\Delta$) and small solvent ($R = 0.5\Delta$) cases. The small solvent case is shown as inset figure. The membrane has the same characteristics as the one shown in Fig. 2. The correlation functions are shown for two different temperatures: very high, $T = 100\epsilon/k_B$ (solid line) and low, $T = 0.1\epsilon/k_B$ (dotted line), as indicated. The data shown for each temperature are calculated from 100 statistically independent conformations sampled in parallel tempering Monte Carlo simulations under equilibrium conditions. The oscillation in the correlation function for small solvent size at low temperature reflects the folding along a preferential axis. Note that in the large solvent case, the correlation, at fixed distance, is larger as temperature decreases demonstrating a stiffening of the membrane due to local crinkling.

correspond to a folded membrane in a dimensionally reduced representation. For sufficiently small solvent size, the ground state of the system is akin to a rolled carpet (Fig. 4c).

Using simple analytic calculations, we find that when $R > \Delta(2 - b^2/\Delta^2)$, a ribbon can adopt a virtually straight conformation with local crinkling that buries the perimeter completely. Such a conformation is shown in Fig. 4a for $R = 2\Delta$ (the buried fraction does not reach 1 only because of edge effects). In an optimal local crinkled conformation, the radius of curvature is equal to Δ at all points. In the continuum, one can approximate a crinkled conformation of the ribbon axis as being formed by joining semicircles of radius Δ , the first convex upwards, the second concave upwards, and so on. The buried fraction of such a continuum crinkled ribbon is given by $f = 1 - (2/\pi) \arcsin\left(\frac{2}{2+R/\Delta}\right)$, which converges to 1 as $R/\Delta \rightarrow \infty$.

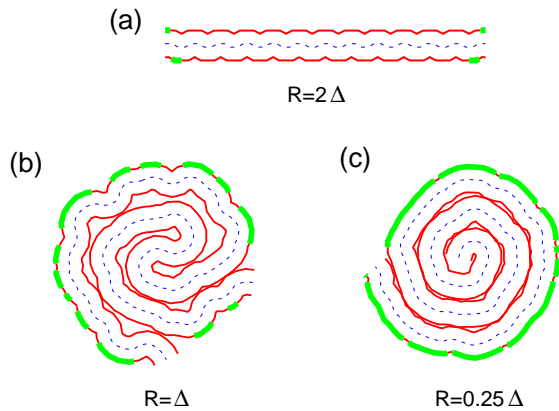


FIG. 4: Conformations of a solvophobic ribbon in 2-D in the presence of a solvent. In the regime where the membrane is folded (Fig. 2) this is a simpler (dimensionally reduced) representation. The ribbons shown are of thickness 2Δ and length $L = 25\Delta$ (a) and $L = 75\Delta$ (b, c). The solvent is comprised of circular discs of radius R whose value is indicated. The ribbon axes are shown as dashed lines. The ribbon perimeters are shown in thinner (thicker) solid line depending on whether they are buried from (exposed to) the solvent. The buried fractions are 0.94 (a), 0.82 (b), and 0.72 (c) for the three cases shown. Conformations (b) and (c) are the ground states obtained in Monte Carlo simulations that seek to minimize the exposed perimeter of the ribbons. Conformation (c) corresponds to the familiar rolled carpet conformation of membranes in 3-D in which the normal vectors lie isotropically within the plane perpendicular to the folding axis.

MEMBRANE NEAR A WALL

We have also studied the behavior of a tethered membrane of *non-zero thickness* near a wall which provides a new mechanism for burying the area of a membrane adsorbed on it. For small solvent molecule size, there is a competition between the binding to the wall and folding for reducing the exposed area. Our simulations show that below a temperature, which increases with membrane size, and is higher than the folding temperature, the membrane is adsorbed on the wall (Fig. 5). An adsorbed membrane would be flat at intermediate temperatures and folded at lower temperatures. Similar considerations suggest that multiple hydrophobic membranes would adhere to each other, at any temperature, to shield much of the surface from the solvent yielding an effectively rigid assemblage of membranes. For large solvent molecules, the adsorption happens below a temperature, that is higher than the temperature of effective local crinkling. At very low temperatures, the membrane is crinkled while remaining bound to the wall.

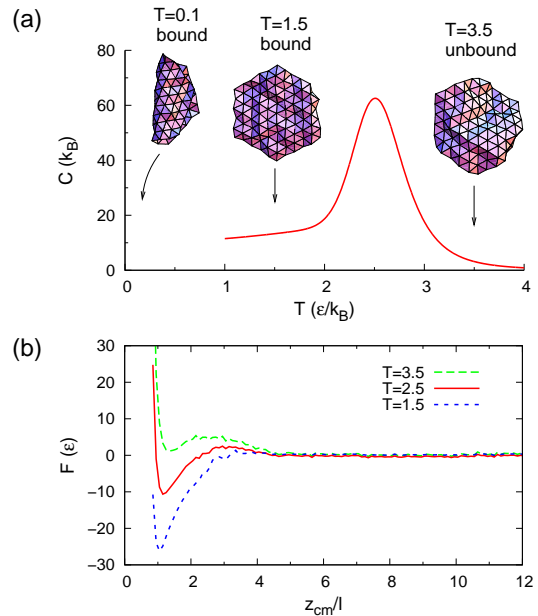


FIG. 5: Adsorption of a membrane on the wall. (a) Temperature dependence of the specific heat for the system of a hydrophobic membrane and a wall. The membrane is hexagonal in shape and has the edge length $L = 5l$ and the thickness $2\Delta = 1.2l$. The solvent radius is $R = \Delta/2$. Adsorption is induced by the shielding of membrane surface from the solvent when it is found near the wall. The adsorption transition is observed at temperature $T \approx 2.5 \epsilon/k_B$. Membrane conformations are shown for selected temperatures as indicated. Both the bound and unbound states at intermediate and high temperatures are flat. The ground state however is a folded membrane bound to the wall, and can be found only at very low temperatures ($T = 0.1 \epsilon/k_B$). (b) The dependence of the effective free energy, F , on the distance, z_{cm} , of the membrane center of mass to the wall for three temperatures: above, below and at the adsorption transition as indicated. The effective free energy is calculated as $F(T, z_{cm}) = -k_B T \ln P(T, z_{cm})$, where $P(T, z_{cm})$ is the probability of finding the membrane at the distance z_{cm} of its center of mass to the wall at temperature T .

DISCUSSION

Previous computational studies of membranes have considered, in essence, models in the infinitesimal thickness limit or 2-d array of spherical particles. The key finding of studies of traditional models (for a review see Ref.[3]) is that a self-avoiding tethered membrane always exists in a flat phase even without any bending rigidity [14–16]. The inclusion of self-attraction [17] leads to several folded phases at intermediate temperatures along with hints of a crumpled phase [18] and an isotropic collapsed phase at low temperatures. A recent study [19] with a Lennard-Jones potential yielded folded sheets and cylindrical conformations. The crumpled state has been also studied for an elastic sheet confined in an im-

penetrable sphere [20] or folded under external forces [21]. Studies of self-intersecting membranes (or phantom membranes) predict a crumpled phase in which the membrane's radius of gyration, R_g , grows as $\sqrt{\ln L}$, where L is the membrane's linear size [22, 23]. With an increase in bending rigidity, phantom membranes undergo a second-order transition from the crumpled phase to the flat phase [24, 25]. The flat, crumpled, and collapsed phases have been observed experimentally in red cell membrane skeletons [26], graphite oxide membrane [27], and molybdenum disulfide [28].

Here we show that incorporating non-zero thickness yields qualitatively new behavior of a hydrophobic membrane seeking to minimize the area exposed to the surrounding solvent molecules. Our simulations show that in the small solvent molecule regime, the thickness of the membrane introduces a spontaneous symmetry breaking within the plane of the membrane. The folding of the membrane occurs multiple times along a dominant folding axis. This is akin to the everyday experience of the greater ease of folding a sheet of paper in a fluted manner compared to first folding the paper along one axis followed by folding the now two layered sheet along a perpendicular axis and so on. A rolled carpet conformation is also effective in burying much of the surface from the solvent molecules (Fig. 4c). Note that the folded structures obtained here are similar to the those in the tubule phase [29] – even in the absence of any anisotropic bending energy, we observe spontaneous symmetry breaking. For a large membrane, one obtains uncoordinated folding at the edges into metastable conformations. The structures of the folded thick membrane are qualitatively similar to those observed in molybdenum disulfide films [28] and in folding of viscous sheets and filaments [30].

For large solvent molecules, the local crinkling mechanism effectively shields the surfaces of the membrane from the solvent, while preserving the overall flat topology. Similar local deformations are observed in real membranes. Wrinkled rigid structures have been observed experimentally upon cooling partially polymerized phospholipid membranes [31] and have been interpreted as resulting from quenched curvature disorder leading to a glassy phase. Studies of wrinkled patterns of polymer films [32] have indicated that thickness plays a role in the formation of these patterns.

We note that the our study considers paint brush sizes in two distinct regimes: smaller than or larger than the membrane thickness. Membranes thicker than the size of a water molecule ($\approx 2.8\text{\AA}$) are quite common. The other limit is obtained when the role of solvent is played by large complexes such as proteins (3-10 nm), t-RNA (7 nm), antibodies (12 nm) and ribosomes (20-30 nm). Interestingly, for a relatively dilute concentration of these complexes, even of the order of 10% in volume fraction according to Asakura-Oosawa theory [33], the entropy depletion effect alone is sufficient to create a tendency

to fold the membrane leading to minimization of the exposed area.

We are indebted to Mehran Kardar, Tom Lubensky, and Michael Plischke for useful comments on the manuscript. This article was supported by the Vietnam National Foundation for Science and Technology Development (NAFOSTED) grant 103.01-2010.11 and Prin 2007.

-
- [1] Nelson D.R. *Statistical Mechanics of Membranes and Surfaces*, 2nd edition, D.R. Nelson T. Piran, World Scientific, Singapore (2004).
 - [2] Lipowsky R. Sackmann E. *Structure and Dynamics of Membranes: I. From Cells to Vesicles & II. Generic and Specific Interaction*, Elsevier, Amsterdam (1995).
 - [3] Wiese K.J. *Phase transitions and critical phenomena*. Domb C. Lebowitz J. Vol. 19 Academic Press, London (2001) pp.253-480.
 - [4] Banavar J.R., Gonzalez O., Maddocks J.H. Maritan A. *J. Stat. Phys.* 110 (2003) 35.
 - [5] Maritan A., Micheletti C., Trovato A. Banavar J.R. *Nature* 406 (2000) 287.
 - [6] Marenduzzo D., Flammini A., Trovato A., Banavar J.R. Maritan A. *J. Polym. Sci.* 43 (2005) 650.
 - [7] Banavar J.R., Hoang T.X., Maddocks J.H., Maritan A., Poletto C., Stasiak A. Trovato A. *Proc. Natl. Acad. Sci. USA* 44 (2007) 17283.
 - [8] Gonzalez O. Maddocks J.H. *Proc. Natl. Acad. Sci. USA* 96 (1999) 4769.
 - [9] Magee J.E., Vasquez V.R. Lue L. *Phys. Rev. Lett.* 96 (2006) 207802.
 - [10] Banavar J.R., Cieplak M., Hoang T.X. Maritan A. *Proc. Natl. Acad. Sci. USA* 106 (2009) 6900.
 - [11] Hadwiger H. *Vorlesungen ber Inhalt, Oberflche und Isoperimetrie*, Springer, Berlin (1957)
 - [12] Hansen-Goos H., Roth R., Mecke K. Dietrich S. *Phys. Rev. Lett.* 99 (2007) 128101.
 - [13] Snir Y. Kamien R.D. *Science* 307 (2005) 1067.
 - [14] Bowick M.J., Cacciuto A., Thorleifsson G. Travesset A. *Eur. Phys. J. E* 5 (2001) 149.
 - [15] Abraham F.F., Rudge W.E. Plischke M. *Phys. Rev. Lett.* 62 (1989) 1757.
 - [16] Grest G.S. *J. Phys. I* 1 (1991) 1695.
 - [17] Abraham F.F. Kardar M. *Science* 252 (1991) 419.
 - [18] Liu D. Plischke M. *Phys. Rev. A* 45 (1992) 7139.
 - [19] Knauert S.T., Douglas J.F. Starr F.W. *Macromolecules* 43 (2010) 3438.
 - [20] Lobkovsky A., Gentges S., Li H., Morse D. Witten T.A. *Science* 270 (1995) 1482.
 - [21] Vlienghart G.A. Gompper G. *Nature Materials* 5 (2006) 216.
 - [22] Gross D.J. *Phys. Lett. B* 138 (1984) 185.
 - [23] Duplantier B. *Phys. Lett. B* 141 (1984) 239.
 - [24] Kantor Y. Nelson D.R. *Phys. Rev. Lett.* 58 (1987) 2774.
 - [25] Aronovitz J.A. Lubensky T.C. *Phys. Rev. Lett.* 60 (1988) 2634.
 - [26] Schmidt C.F., Svoboda K., Lei N., Petsche I.B., Berman L.E., Safinya C.R. Grest G.S. *Science* 259 (1993) 952.
 - [27] Wen X., Garland C.W., Hwa T., Kardar M., Kokufuta

- E., Li Y., Orkisz M. Tanaka T. Nature 355 (1992) 426.
- [28] Chianelli R.R., Prestridge E.B., Pecoraro T.A. DeNeufville J.P. Science 203 (1979) 1105.
- [29] Radzihovsky L. Toner J. Phys. Rev. Lett. 75 (1995) 4752.
- [30] Skorobogatiy M. Mahadevan L. Europhys. Lett. 52 (2000) 532.
- [31] Mutz M., Bensimon D. Brienne M.J. Phys. Rev. Lett. 67 (1991) 923.
- [32] Huang J., Juskiewicz M., de Jeu W. H., Cerda E., Emrick T., Menon N. Russell T.P. Science 317 (2007) 650.
- [33] Asakura S. Oosawa F. J. Polym. Sci. 33 (1958) 183.